

# Resilient Disaster Recovery Logistics of Distribution Systems: Co-Optimize Service Restoration with Repair Crew and Mobile Power Source Dispatch

Shunbo Lei, *Member, IEEE*, Chen Chen, *Member, IEEE*, Yupeng Li, *Member, IEEE*,  
and Yunhe Hou, *Senior Member, IEEE*

**Abstract**—Repair crews (RCs) and mobile power sources (MPSs) are critical resources for distribution system (DS) outage management after a natural disaster. However, their logistics is not well investigated. We propose a resilient scheme for disaster recovery logistics to co-optimize DS restoration with dispatch of RCs and MPSs. A novel co-optimization model is formulated to route RCs and MPSs in the transportation network, schedule them in the DS, and reconfigure the DS for microgrid formation coordinately, etc. The model incorporates different timescales of DS restoration and RC/MPS dispatch, the coupling of transportation and power networks, etc. To ensure radiality of the DS with variable physical structure and MPS allocation, we also model topology constraints based on the concept of spanning forest. The model is convexified equivalently and linearized into a mixed-integer linear programming. To reduce its computation time, preprocessing methods are proposed to pre-assign a minimal set of repair tasks to depots and reduce the number of candidate nodes for MPS connection. Resilient recovery strategies thus are generated to enhance service restoration, especially by dynamic formation of microgrids that are powered by MPSs and topologized by repair actions of RCs and network reconfiguration of the DS. Case studies demonstrate the proposed methodology.

**Index Terms**—Disaster recovery logistics, distribution system, mobile power sources, repair crews, resilience.

## I. INTRODUCTION

RECENT years have witnessed more frequent natural disasters causing severe power outages, which result in tremendous economic loss, etc. The urgency to enhance power grid resilience is highlighted. Specifically, efficient outage management is one of the critical requirements for resilient power grids.

Repair crews (RCs) are crucial response resources for power grid outage management against natural disasters. It is desired that they repair damaged components in an optimal order. Mobile power sources, including truck-mounted mobile emergency generators (MEGs) [1], mobile energy storage systems (MESSs) [2], are also important flexibility resources for grid restoration. They can supply critical loads that lose access to the main grid

This work was supported in part by the National Natural Science Foundation of China under Grant 51677160, and in part by the Research Grant Council of Hong Kong SAR through the Theme-based Research Scheme under Project No. T23-701/14-N. The work of C. Chen was supported by the U.S. Department of Energy (DOE)'s Office of Electricity Delivery and Energy Reliability.

S. Lei and Y. Hou are with the Department of Electrical and Electronic Engineering, The University of Hong Kong, Hong Kong; Y. Hou is also with The University of Hong Kong Shenzhen Institute of Research and Innovation, Shenzhen 518057, China (email: leishunbo@eee.hku.hk, yhou@eee.hku.hk).

C. Chen is with the Energy Systems Division, Argonne National Laboratory, Argonne, IL 60439 USA (email: morningchen@anl.gov).

Y. Li is with the Department of Computer Science, The University of Hong Kong, Hong Kong (email: ypli@connect.hku.hk).

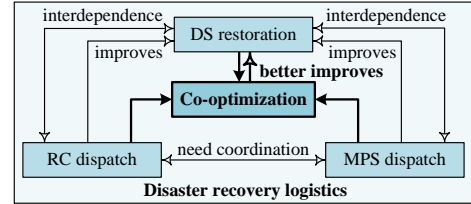


Fig. 1. Relationships among DS restoration, RC dispatch and MPS dispatch.

power. As for power grids, i.e., distribution systems (DSs) in this work, their restoration involves many decisions and different strategies, e.g., forming microgrids by network reconfiguration [3][4]. Integrating these elements (see Fig. 1), DS outage management becomes a *disaster recovery logistics* problem to route RCs and MPSs in the transportation network [5], schedule them in the DS, and reconfigure the DS, etc., for electric service restoration. Involving different resources and infrastructures, this problem is currently not well investigated.

As depicted in Fig. 1, the 3 sub-problems are interdependent. Coordination is required to better improve service restoration. References [6][7] review the dispatch and planning of RCs in DSs. Their interdependence is often simplified or ignored, e.g., in [8]. Only several publications, e.g., [9], co-optimize RC dispatch with DS restoration. As for MPSs, in [10], [11] and [12], MESSs are dispatched to reduce DS operation cost, improve reliability, and enhance preparedness against natural disasters, respectively. Review on MEGs can be found in [13]. In general, MPS dispatch is seldomly co-optimized with DS restoration, and never in a dynamic manner. Besides, no publication has considered both RCs and MPSs for DS service restoration.

This paper proposes a co-optimization method for DS disaster recovery logistics. RC dispatch and MPS dispatch are jointly coordinated with DS restoration to better enhance grid resilience. A non-convex mixed-integer non-linear programming (MINLP) model is formulated to co-optimize the routing and scheduling of RCs and MPSs, dynamic microgrid formation of the DS, etc. Issues such as different timescales of RC/MPS dispatch and DS restoration, the coupling of transportation and power networks, MESSs' state of charge (SoC) variations over time, and radiality constraints for a DS with variable physical structure and MPS allocation, are resolved. The model is equivalently convexified as a mixed-integer second-order cone programming (MISCOP) and further linearized to be a mixed-integer linear programming (MILP). Preprocessing methods, e.g., pre-assigning minimum repair tasks, are also proposed to reduce its computation time.

In the following, Section II, III and IV formulate RC dispatch, MPS dispatch and DS restoration, respectively. Section V builds the co-optimization model. Section VI, VII and VIII present the solution method, case studies and conclusion, respectively.

## II. ROUTING AND SCHEDULING OF RCS

Dispatch of RCs involves two interdependent sub-tasks, i.e., routing and scheduling. Routing is to select a route for each RC to travel among depots and damaged components. Scheduling is to set a timetable for RCs' traveling and repairing behaviors.

Let  $V \triangleq V_1 \cup V_2$  be the set of damaged components ( $V_1$ ) and depots ( $V_2$ ). Let  $A \triangleq \{(m, n), \forall m, n \in V\}$  be the set of edges for all pairs of vertices. Then, the routing of RCs is to find their optimal paths in graph  $G \triangleq (V, A)$ . As the routing problem can be seen as a generalization of the traveling salesman problem (TSP) [14], its modeling is normally based on the TSP formulation, e.g., in [9]. Here we propose a model much simpler and more appropriate for the studied problem.

The TSP formulation is based on edge-wise routing variables  $a_{mn}^k$  (1 if RC  $k$  travels edge  $(m, n)$ , 0 otherwise). In this work, we use vertex-wise variables  $a_{m,t}^k$  instead (1 if RC  $k$  is at vertex  $m$  at time  $t$ , 0 otherwise). Note that with subscript  $t$ ,  $a_{m,t}^k$  are actually scheduling variables. We will show that the routing problem can be incorporated using  $a_{m,t}^k$  only.

In scheduling RCs, each RC  $k$  can only be visiting at most one vertex at each time  $t$ :

$$\sum_{m \in V} a_{m,t}^k \leq 1, \forall k, \forall t. \quad (1)$$

For conciseness of the objective function to be modeled in Section V, auxiliary variables  $\beta_t^k$  are introduced:

$$\beta_t^k = 1 - \sum_{m \in V} a_{m,t}^k, \forall k, \forall t. \quad (2)$$

If RC  $k$  is traveling on the transportation network at time  $t$ ,  $\beta_t^k = 1$ ; if it is visiting one of the vertices,  $\beta_t^k = 0$ .

The routing of RCs imposes travel time constraints on RC scheduling. For example, if RC  $k$  is at vertex  $m$  at time  $t = 1$  (i.e.,  $a_{m,1}^k = 1$ ), and it takes 2 time periods to travel from vertex  $m$  to  $n$ , then RC  $k$  is possible at vertex  $n$  only after  $t = 3$  (i.e.,  $a_{n,2}^k = a_{n,3}^k = 0$ ). Such constraints are modeled as:

$$a_{n,t+\tau}^k + a_{m,t}^k \leq 1, \forall k, \forall m \neq n, \forall \tau \leq tr_{mn}, \forall t \leq T - \tau. \quad (3)$$

where  $tr_{mn}$  is the travel time between vertices  $m$  and  $n$ ; and  $T$  is the number of time periods. Note that (3) actually includes (1) implicitly with  $\tau = 0$ . To reduce the number of constraints, (3) can also be equivalently transformed into:

$$\sum_{\tau=t+1}^{\min(t+tr_{mn}, T)} a_{n,\tau}^k \leq (1 - a_{m,t}^k) \cdot \min(tr_{mn}, T - t), \quad (4)$$

$$\forall k, \forall m \neq n, \forall t.$$

Actually, (3) or (4) is all we need to incorporate the routing sub-problem in the co-optimization. Other routing constraints, e.g., path-flow balance, will be satisfied implicitly. The validity of (3) and (4) is supported by the following proposition:

*Proposition 1:* For any RC scheduling plan satisfying (3) or (4), there exists at least one corresponding feasible path in  $G$ .

The proof of Proposition 1 is straightforward. The key is that we can use  $a_{m,t}^k$  to retrieve the path of RC  $k$  simply by:

$$\begin{bmatrix} a_{1,1}^k & \cdots & a_{V,1}^k \\ \vdots & \ddots & \vdots \\ a_{1,T}^k & \cdots & a_{V,T}^k \end{bmatrix} \cdot \begin{bmatrix} 1 \\ \vdots \\ V \end{bmatrix} \quad (5)$$

where  $V$  is the cardinality of  $V$ .

The advantages of our proposed model for the routing sub-problem are mainly twofold: 1) The issues of transportation-DS networks coupling and their different timescales are resolved in a simpler manner compared with the common TSP formulation. 2) It does not enforce RCs to visit all vertices of damaged components ( $V_1$ ). Thus, in the co-optimization, we can repair a minimal set of damaged components to restore all loads.

Next, we formulate the repair plan, which depends on the routing and scheduling of RCs. Let  $z_{m,t}^k$  be 1 if damaged component  $m$  is repaired by RC  $k$  at time  $t$ , 0 otherwise. Let  $rt_m^k$  be the required time periods for RC  $k$  to repair damaged component  $m$ . Then, we have:

$$z_{m,t}^k \leq \frac{\sum_{\tau=1}^t a_{m,\tau}^k}{rt_m^k}, \forall k, \forall m \in V_1, \forall t. \quad (6)$$

$$z_{m,t}^k \leq z_{m,t+1}^k, \forall k, \forall m \in V_1, \forall t \leq T - 1. \quad (7)$$

For example, if it takes  $rt_m^k = 2$  time periods of RC  $k$  to repair damaged component  $m$ , and RC  $k$  repairs it at time  $t = 1 \sim 2$  (i.e.,  $[a_{m,1}^k, a_{m,2}^k] = [1, 1]$ ), then according to (6) we have  $z_{m,1}^k \leq \frac{1}{2}$  and  $z_{m,2}^k \leq \frac{1+1}{2}$ . As  $z_{m,t}^k$  is binary, we further have  $[z_{m,1}^k, z_{m,2}^k, \dots, z_{m,T}^k] = [0, 1, \dots, 1]$ . Note that decisions such as  $[a_{m,1}^k, a_{m,2}^k, a_{m,3}^k] = [1, 0, 1]$  (idling the RC at  $t = 2$  during the repair) and  $[a_{m,1}^k, a_{m,2}^k, a_{m,3}^k] = [1, 1, 1]$  (idling the RC at  $t = 3$  after the repair) are also feasible in (6). However, such decisions are not optimal. They will be eliminated when solving the co-optimization problem.

The following constraints state that each damaged component is repaired only once by one of the RCs:

$$\sum_k z_{m,t}^k \leq 1, \forall m \in V_1, \forall t. \quad (8)$$

Actually, (8) is dispensable. Without it, the co-optimization also seeks an optimal solution without repeated repairs. Nevertheless, with (8), the linear programming relaxation of our MILP co-optimization model is tightened. It helps to reduce the solution time using MILP solvers that are generally based on the branch-and-bound framework [15].

The following constraints enforce that RC  $k$ 's resource capacity suffices the total resources required by its repair tasks:

$$\sum_{m \in V_1} z_{m,T}^k \cdot rs_m \leq RS^k, \forall k. \quad (9)$$

where  $rs_m$  is the number of resources required to repair damaged component  $m$ ; and  $RS^k$  is RC  $k$ 's resource capacity.

## III. ROUTING AND SCHEDULING OF MPSS

Dispatch of MPSSs also involves two interdependent sub-tasks, i.e., routing and scheduling. Routing is to select a route for each MPSS to travel among candidate nodes for MPSS connection

in the DS. Scheduling is to manage MPSs' traveling behaviors and power outputs (or inputs for MESSs when charging) over the considered time window.

Let  $\mathcal{N}$  be the set of DS nodes; and  $\mathcal{N}' \subset \mathcal{N}$  be the set of candidate nodes for MPS connection. Let  $\mathcal{M}_1$  be the set of MEGs;  $\mathcal{M}_2$  be the set of MESSs; and  $\mathcal{M} \triangleq \{\mathcal{M}_1 \cup \mathcal{M}_2\}$  be the set of MPSs. Let  $vol_i$  be the allowed number of MPSs connected to node  $i$ . Similar to the RC dispatch model, let  $\alpha_{i,t}^s$  be 1 if MPS  $s$  is connected to node  $i$  at time  $t$ , 0 otherwise. Then, we have:

$$\sum_{i \in \mathcal{N}'} \alpha_{i,t}^s \leq 1, \forall s, \forall t. \quad (10)$$

$$\begin{aligned} \min(t+tr_{ij}, T) \\ \sum_{\tau=t} \alpha_{j,\tau}^s \leq (1 - \alpha_{i,t}^s) \cdot \min(tr_{ij}, T - t), \end{aligned} \quad (11)$$

$$\forall s, \forall i \in \mathcal{N}', \forall j \in \mathcal{N}' \setminus \{i\}, \forall t.$$

$$\sum_{s \in \mathcal{M}} \alpha_{i,t}^s \leq vol_i, \forall i \in \mathcal{N}', \forall t. \quad (12)$$

Above, (10) and (11) are essentially the same as (1) and (4), respectively; and (12) limits the number of MPSs connected to each candidate node by its capacity. The routing and traveling behaviors of MPSs are sufficiently formulated by (10)-(12). Again, for conciseness of the objective function to be modeled in Section V, auxiliary variables  $\beta_t^s$  are introduced:

$$\beta_t^s = 1 - \sum_{i \in \mathcal{N}'} \alpha_{i,t}^s, \forall s, \forall t. \quad (13)$$

That is,  $\beta_t^s = 1$  if MPS  $s$  is traveling on the transportation network at time  $t$ ;  $\beta_t^s = 0$  if it is connected to the DS.

Next, we formulate the power dispatch of MPSs. First, for MEGs, let  $gp_t^s$  and  $gq_t^s$  be the real and reactive power output of MEG  $s$  at time  $t$ , respectively; let  $\overline{gp}^s$  and  $\overline{gq}^s$  be the maximum real and reactive power output of MEG  $s$ , respectively. Then, the following constraints are enforced:

$$0 \leq gp_t^s \leq \sum_{i \in \mathcal{N}'} \alpha_{i,t}^s \cdot \overline{gp}^s, \forall s \in \mathcal{M}_1, \forall t. \quad (14)$$

$$0 \leq gq_t^s \leq \sum_{i \in \mathcal{N}'} \alpha_{i,t}^s \cdot \overline{gq}^s, \forall s \in \mathcal{M}_1, \forall t. \quad (15)$$

With (14) and (15), MEGs' power outputs are restricted by their capacities, and enforced to be zero if a MEG is not connected to the DS. Fuel limits of MEGs are not included, as they can be refueled by tanker trucks in case of long-term blackouts [16].

Second, for MESSs, let  $c_t^s$  and  $d_t^s$  be 1 if MESS  $s$  is charging and discharging at time  $t$ , respectively, 0 otherwise; let  $cp_t^s$  and  $dp_t^s$  be the charging and discharging power of MESS  $s$  at time  $t$ , respectively; let  $\overline{cp}^s$  and  $\overline{dp}^s$  be the maximum charging and discharging power of MESS  $s$ , respectively; let  $soc_t^s$  be the SoC of MESS  $s$  at time  $t$ ; let  $\eta_s^c$  and  $\eta_s^d$  be the charging and discharging efficiency of MESS  $s$ , respectively; let  $\underline{soc}^s$  and  $\overline{soc}^s$  be the minimum and maximum SoC of MESS  $s$ , respectively. Then, the following constraints are enforced:

$$c_t^s + d_t^s \leq \sum_{i \in \mathcal{N}'} \alpha_{i,t}^s, \forall s \in \mathcal{M}_2, \forall t. \quad (16)$$

$$0 \leq cp_t^s \leq c_t^s \cdot \overline{cp}^s, \forall s \in \mathcal{M}_2, \forall t. \quad (17)$$

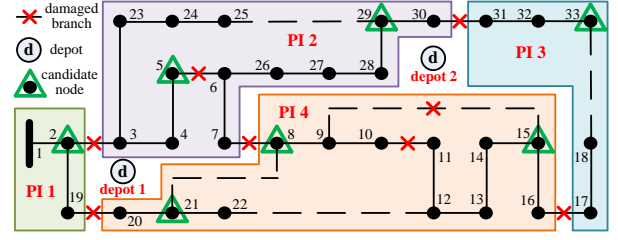


Fig. 2. IEEE 33-node test system split into multiple PIs.

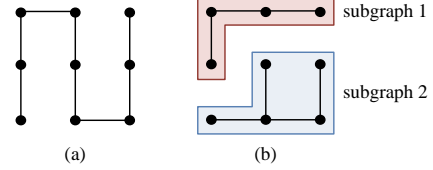


Fig. 3. (a) A spanning tree; (b) A spanning forest.

$$0 \leq dp_t^s \leq d_t^s \cdot \overline{dp}^s, \forall s \in \mathcal{M}_2, \forall t. \quad (18)$$

$$0 \leq gq_t^s \leq (c_t^s + d_t^s) \cdot \overline{gq}^s, \forall s \in \mathcal{M}_2, \forall t. \quad (19)$$

$$\begin{aligned} soc_{t+1}^s = soc_t^s + (cp_t^s \cdot \eta_s^c - \frac{dp_t^s}{\eta_s^d}) \cdot \Delta t, \\ \forall s \in \mathcal{M}_2, \forall t \leq T - 1. \end{aligned} \quad (20)$$

$$\underline{soc}^s \leq soc_t^s \leq \overline{soc}^s, \forall s \in \mathcal{M}_2, \forall t. \quad (21)$$

where  $\Delta t$  is the duration of one time period. Specifically, (16) ensures that in each time period, charging and discharging are mutually exclusive states of a MESS, and it can neither charge nor discharge if it is not connected to the DS; (17) and (18) specify MESSs' charging and discharging power limits, respectively (if a MESS is not in the charging/discharging state, its charging/discharging power is limited to be zero); (19) is similar to (15); (20) expresses MESSs' SoC variations over time; and (21) imposes SoC ranges for MESSs.

#### IV. DYNAMIC NETWORK RECONFIGURATION AND POWER DISPATCH OF THE DS

To coordinate with RC/MPS dispatch, DS is dynamically reconfigured, e.g., to form microgrids. DS topology has to be radial in this process. As researchers have extensively studied DS reconfiguration, the modeling of radiality constraints is resolved to some extent. However, in this work we encounter a new situation: The physical structure of the DS varies with the repair plan, and the source node distribution in the DS varies with the allocation of MPSs. In general, we are reconfiguring a variable DS. For example, a natural disaster split the DS in Fig. 2 into 4 physical islands (PIs). Then, at some future time  $t$  of the recovery process, the number of PIs, the components of each PI, etc., are all variables that are not only dependent on but also to be co-optimized with RC and MPS dispatch decisions. Existing methods to formulate radiality constraints in the literature are not applicable in this case.

Different from common DS reconfiguration problems that seek an optimal *spanning tree* (a radial topology connecting all nodes without loops), in this work, with PIs, each feasible topology is a *spanning forest* (each subgraph being a spanning tree; see Fig. 3). Recent publications [3] and [4] on microgrids formation are essentially constructing a spanning forest, too.

However, their models are neither applicable here. Also note that [9] is essentially reconfiguring a variable DS. It uses the constraints from [17] to ensure radiality. However, a topology satisfying such constraints is not necessarily radial [18].

Observing the difference and connection between spanning tree and spanning forest, we propose the following method to express radiality constraints for a variable DS. For the DS network, let  $\lambda_t^{ij}$  be the connection status of branch  $(i, j)$  at time  $t$  (1 if closed, 0 if open); let  $u_t^{ij}$  be the operable status of branch  $(i, j)$  at time  $t$  (1 if can be used, 0 if damaged and unrepaired). Introduce another fictitious network the same as the DS network but without damages. Let  $e_t \triangleq \{e_t^{ij}, \forall(i, j)\}$  be connection status of the fictitious network at time  $t$ . Then, radiality constraints of our studied problem is expressed as:

$$(22a) : e_t \in \Omega, \forall t; \quad (22b) : \lambda_t^{ij} \leq e_t^{ij}, \forall(i, j), \forall t; \quad (22) \\ (22c) : \lambda_t^{ij} \leq u_t^{ij}, \forall(i, j), \forall t.$$

where  $\Omega$  is the set of spanning tree topologies of the fictitious network. Note that (22a) can be easily formulated by constraints based on the single-commodity flow model [19], which have been used extensively. For space limit, we do not expand on the explicit formulation of (22a), and only write it symbolically here. In general, (22a) requires  $e_t$  to form a fictitious spanning tree; (22b) restricts the DS to close only a subset of the branches in the fictitious spanning tree; and (22c) enforces inoperable branches to be open. With (22),  $\lambda_t \triangleq \{\lambda_t^{ij}, \forall(i, j)\}$  forms a spanning forest in each time period.

The validity of (22) is supported by the following property: removing  $l \geq 0$  edges from a spanning tree leads to a spanning forest. In other words, subgraphs of a spanning tree are also spanning trees, thus forming a spanning forest.

Next, we model power dispatch of the DS. Let  $\delta_t^i$  be 1 if the load at node  $i$  is restored at time  $t$ , 0 otherwise; let  $p_t^i$  and  $q_t^i$  be the real and reactive power demand of node  $i$  at time  $t$ , respectively; let  $P_t^i$  and  $Q_t^i$  be the real and reactive power output of the MPS(s) at node  $i$  at time  $t$ , respectively; let  $v_t^i$  be the squared voltage magnitude of node  $i$  at time  $t$ ; let  $\underline{v}^i$  and  $\bar{v}^i$  be the minimum and maximum voltage value of node  $i$ , respectively; let  $pf_t^{ij}$  and  $qf_t^{ij}$  be the real and reactive power flow on branch  $(i, j)$  at time  $t$ , respectively; let  $r_{ij}$ ,  $x_{ij}$  and  $\bar{S}_{ij}$  be the resistance, reactance and apparent power capacity of branch  $(i, j)$ , respectively. Then, we have:

$$\delta_t^i \leq \delta_{t+1}^i, \forall i, \forall t \leq T - 1. \quad (23)$$

$$P_t^i - \delta_t^i \cdot p_t^i + \sum_{(j,i) \in \mathbf{L}} pf_t^{ji} - \sum_{(i,j) \in \mathbf{L}} pf_t^{ij} = 0, \forall i, \forall t. \quad (24)$$

$$Q_t^i - \delta_t^i \cdot q_t^i + \sum_{(j,i) \in \mathbf{L}} qf_t^{ji} - \sum_{(i,j) \in \mathbf{L}} qf_t^{ij} = 0, \forall i, \forall t. \quad (25)$$

$$(\underline{v}^i)^2 \leq v_t^i \leq (\bar{v}^i)^2, \forall i, \forall t. \quad (26)$$

$$(pf_t^{ij})^2 + (qf_t^{ij})^2 \leq \lambda_t^{ij} \cdot (\bar{S}_{ij})^2, \forall(i, j), \forall t. \quad (27)$$

$$v_t^i - v_t^j \leq (1 - \lambda_t^{ij}) \cdot K + 2 \cdot (r_{ij} \cdot pf_t^{ij} + x_{ij} \cdot qf_t^{ij}), \quad (28) \\ \forall(i, j), \forall t.$$

$$v_t^i - v_t^j \geq (\lambda_t^{ij} - 1) \cdot K + 2 \cdot (r_{ij} \cdot pf_t^{ij} + x_{ij} \cdot qf_t^{ij}), \quad (29) \\ \forall(i, j), \forall t.$$

where  $\mathbf{L}$  is the set of DS branches; and  $K$  is a large enough positive number. As above, (23) prevent de-energizing loads that are already restored; (24) and (25) require all nodes to satisfy real and reactive power balance conditions, respectively; (26) specifies voltage magnitude limits; (27) limit the apparent power on each branch by its capacity, and restrict both real and reactive power flow on a branch to be zero if it is open; (28) and (29) represent the power flow equation based on the DistFlow model [20] [21] for closed branches with  $\lambda_t^{ij} = 1$ , and get relaxed for open branches with  $\lambda_t^{ij} = 0$ .

Thus, with (22)-(29), dynamic network reconfiguration and power dispatch of the DS are coordinated to achieve service restoration via strategies such as microgrid formation.

## V. THE CO-OPTIMIZATION MODEL

DS service restoration is co-optimized with RC dispatch and MPS dispatch to enhance DS resilience. Let  $\omega^i$  be the priority weight of the power demand at node  $i$ . The objective function of the co-optimization is modeled as follows:

$$\max \sum_t \left[ \sum_i \omega^i \cdot \delta_t^i \cdot q_t^i - \varepsilon \cdot \left( \sum_k \beta_t^k + \sum_s \beta_t^s \right) \right] \quad (30)$$

which maximizes the weighted sum of restored loads over time, and minimizes the total number of travels of RCs and MPSs. Relative weights of the two objectives are adjusted by parameter  $\varepsilon$ , which is set as a small value so that the first objective is still dominating. We add the second objective for two main reasons: 1) To restrict the transportation of RCs and MPSs during time  $t \sim T$  if all loads are restored at some time  $t < T$ ; 2) To select a dispatch strategy achieving the optimal recovery effect by a minimum number of travels of RCs and MPSs.

Next, we model the interdependence among RC dispatch, MPS dispatch and DS service restoration. First, the relationship between RC dispatch and DS restoration is modeled. Let branch  $(i_m, j_m)$  denote the corresponding damaged component  $m$ ; let  $\mathbf{L}_1 \triangleq \{(i_m, j_m), \forall m \in \mathbf{V}_1\}$  be the set of damaged branches; let  $\mathbf{L}_2$  be the set of branches with switches. Then, we have:

$$u_t^{ij} = 1, \forall(i, j) \in \mathbf{L} \setminus \mathbf{L}_1, \forall t. \quad (31)$$

$$u_{t+1}^{i_m j_m} \leq \sum_k z_{m,t}^k, \forall m \in \mathbf{V}_1, \forall t \leq T - 1. \quad (32)$$

$$\lambda_t^{ij} = 1, \forall(i, j) \in \mathbf{L} \setminus \{\mathbf{L}_1 \cup \mathbf{L}_2\}, \forall t. \quad (33)$$

As above, (31) states that an intact branch is always operable; (32) indicates that a damaged branch is operable only if it is repaired by one of the RCs in the previous time period; (33) enforces undamaged branches without switches to be closed.

Second, the relationship between MPS dispatch and DS service restoration is incorporated by the following equations:

$$P_t^i = \sum_{s \in \mathbf{M}_1} \alpha_{i,t}^s \cdot gp_t^s + \sum_{s \in \mathbf{M}_2} \alpha_{i,t}^s \cdot (dp_t^s - cp_t^s), \quad (34) \\ \forall i \in \mathbf{N}', \forall t.$$

$$Q_t^i = \sum_{s \in \mathbf{M}} \alpha_{i,t}^s \cdot gq_t^s, \forall i \in \mathbf{N}', \forall t. \quad (35)$$

$$P_t^i = Q_t^i = 0, \forall i \in \mathbf{N} \setminus \mathbf{N}', \forall t. \quad (36)$$

With (34) and (35),  $P_t^i$  and  $Q_t^i$  are derived by summing the real and reactive power outputs of MPSs connected to node  $i$  at time  $t$ , respectively; (36) enforces  $P_t^i$  and  $Q_t^i$  to be zero for nodes that are not for MPS connection.

Note that although (31)-(36) do not show direct relationship between RC dispatch and MPS dispatch, they are intrinsically interrelated in the studied problem. They need to be coordinated, i.e., co-optimized, to attain better service restoration of the DS.

Thus, we arrive at the co-optimization model as follows:

*Objective* : (30);

*Constraints* : (1), (2), (4), (6)–(29), (31)–(36);

*Variables* :  $a_{m,t}^k, \beta_t^k, z_{m,t}^k$ ;  
 $\alpha_{i,t}^s, \beta_t^s, gp_t^s, gq_t^s, c_t^s, d_t^s, cp_t^s, dp_t^s, soc_t^s$ ;  
 $\delta_t^i, P_t^i, Q_t^i, v_t^i, \lambda_t^{ij}, u_t^{ij}, e_t^{ij}, pf_t^{ij}, qf_t^{ij}$ .

Above, the list of variables are also provided for clarity.

## VI. SOLUTION METHOD

### A. Linearization Techniques

The proposed co-optimization model is a non-convex MINLP, as (34) and (35) have non-linear and non-convex terms such as  $\alpha_{i,t}^s \cdot gp_t^s$ . They are linearized by the McCormick envelopes [22]. As  $\alpha_{i,t}^s$  is binary, and the involved continuous variables have explicit lower and upper bounds, the linearization is equivalent. By doing this, the co-optimization model is also convexified into a MISOCP. We further linearize (27) using the technique in [23]. The co-optimization model thus becomes a MILP, which can be solved by off-the-shelf solvers such as Gurobi. As the involved linearizations are straightforward, we do not elaborate on the detailed reformulations for space limit.

### B. Pre-Assigning a Minimal Set of Repair Tasks to Depots

To reduce the MILP co-optimization model's computational complexity, we follow [9] to cluster and pre-assign repair tasks to depots. Let  $\psi_n^m$  be 1 if damaged component  $m$  is assigned to depot  $n$ , 0 otherwise; let  $l_{mn}$  be the distance between damaged component  $m$  and depot  $n$ ; let  $\Phi_n$  be the set of RCs in depot  $n$ . Then, the pre-assignment of repair tasks to depots is determined by the small MILP model as follows:

$$\min_{\substack{\psi_n^m, u^{ij}, \lambda^{ij}, e^{ij}, \\ pf^{ij}, qf^{ij}, v^i}} \sum_{m \in \mathbf{V}_1} \sum_{n \in \mathbf{V}_2} \psi_n^m \cdot l_{mn} \quad (37)$$

$$s.t. \quad \sum_{m \in \mathbf{V}_1} \psi_n^m \cdot rsm \leq \sum_{k \in \Phi_n} RS^k, \forall n \in \mathbf{V}_2. \quad (38)$$

$$\sum_{n \in \mathbf{V}_2} \psi_n^m \leq 1, \forall m \in \mathbf{V}_1. \quad (39)$$

$$u^{imjm} \leq \sum_{n \in \mathbf{V}_2} \psi_n^m, \forall m \in \mathbf{V}_1. \quad (40)$$

$$\sum_{(j,i) \in \mathbf{L}} pf^{ji} - \sum_{(i,j) \in \mathbf{L}} pf^{ij} - p^i = 0, \forall i. \quad (41)$$

$$\sum_{(j,i) \in \mathbf{L}} qf^{ji} - \sum_{(i,j) \in \mathbf{L}} qf^{ij} - q^i = 0, \forall i. \quad (42)$$

$$(22), (26)–(29), (31), (33) \text{ (without time subscript } t). \quad (43)$$

Specifically, (37) minimizes the sum of distances between damaged components and their assigned depots, so as to reduce the transportation time of RCs and thus enhance DS restoration; (38) requires each depot to have adequate resources to complete its assigned repair tasks; and (39) states that each damaged component is assigned to at most one depot. Note that, different from [9], here we do not demand all tasks to be assigned. The above model just seeks and assigns *a minimal set of repair tasks* that can fully restore all DS loads without MPSs. Thus, (40)-(43) are added: (40) states that a damaged branch will be operable only if it is assigned to be repaired; (41) and (42) represent the power balance conditions to fully supply all loads without MPSs; (43) are the other DS operational constraints. Parameters  $p^i/q^i$  can be set as the maximum power demands of DS nodes. And note that power outputs of the substation are implicitly modeled as  $pf^{i_g^j}/qf^{i_g^j}$ , where  $i_g$  denotes the substation node. Though without the time subscript  $t$ , other involved variables and constraints are introduced hereinbefore. By selecting and assigning a minimal set of repair tasks rather than all tasks to depots, computational complexity of the co-optimization model is further reduced. Another advantage is that, after all loads are restored by a minimal set of repair tasks, RCs can be better scheduled to help recover other DSs.

### C. Selecting Candidate Nodes for MPS Connection

The co-optimization model's computation time also partially depends on the number of candidate nodes for MPS connection in the DS. Here, one candidate node is selected from each PI.

First, we need to find the set of candidate nodes in each PI. Let  $\mathbf{I}$  be the set of all candidate nodes, i.e., nodes meeting the requirements of MPS connection, e.g., facility requirements [13]; let  $\mathbf{I}_\sigma$  be the set of candidate nodes in PI  $\sigma$ ; let  $v2s$  be an operation transforming a vector into a set, e.g.,  $[0, 1, 2] \rightarrow \{0, 1, 2\}$ ; let  $\odot$  be the symbol for Hadamard product, i.e., element-wise multiplication; let  $\Theta$  be the adjacency matrix ( $\Theta_{ij} = 1$  if there is an intact branch  $(i, j)$ , whether closed or open;  $\Theta_{ij} = 0$  otherwise); let  $\Theta_i$  be the  $i$ th row of  $\Theta$ . Algorithm 1 as follows is proposed to find  $\mathbf{I}_\sigma$  for each PI  $\sigma$ :

---

**Algorithm 1** Find the set of candidate nodes in each PI

---

Input:  $\mathbf{N}, \Theta, \mathbf{I}$ ; Output:  $\mathbf{I}_\sigma, \forall \sigma$ .

- 1:  $\sigma \leftarrow 1, \mathcal{N} \leftarrow \emptyset$ ;
  - 2: **while**  $\mathbf{N} \setminus \mathcal{N} \neq \emptyset$  **do**
  - 3:   randomly select  $i \in \mathbf{N} \setminus \mathcal{N}, \mathbf{I}_\sigma \leftarrow \{i\}, \mathcal{I}_\sigma \leftarrow \{i\}$ ;
  - 4:    $\mathbf{C}_i \leftarrow v2s(\Theta_i \odot [1, \dots, N]), \mathbf{I}_\sigma \leftarrow \{\mathbf{I}_\sigma \cup \mathbf{C}_i\} \setminus \{0\}$ ;
  - 5:   **if**  $\mathbf{I}_\sigma \setminus \mathcal{I}_\sigma \neq \emptyset$  **then**
  - 6:     randomly select  $i \in \mathbf{I}_\sigma \setminus \mathcal{I}_\sigma, \mathcal{I}_\sigma \leftarrow \mathcal{I}_\sigma \cup \{i\}$ ;
  - 7:     **go to step 4**;
  - 8:    $\mathcal{N} \leftarrow \mathcal{N} \cup \mathbf{I}_\sigma, \mathbf{I}_\sigma \leftarrow \mathbf{I}_\sigma \cap \mathbf{I}, \sigma \leftarrow \sigma + 1$ ;
  - 9:   **go to step 3**;
- 

Then, the final selection of candidate nodes is determined by the small integer programming (IP) model as follows:

$$\min_{\phi_i} \frac{1}{2} \sum_{\sigma} \sum_{i \in \mathbf{I}_\sigma} \sum_{j \in \mathbf{I} \setminus \mathbf{I}_\sigma} \phi_i \cdot \phi_j \cdot l_{ij} \quad (44)$$

$$s.t. \quad \sum_{i \in \mathbf{I}_\sigma} \phi_i = 1, \forall \sigma \text{ with } \mathbf{I}_\sigma \neq \emptyset. \quad (45)$$

where  $\phi_i = 1$  if candidate node  $i$  is selected,  $\phi_i = 0$  otherwise;  $l_{ij}$  is the distance between nodes  $i$  and  $j$ ;  $I_\sigma$  is the cardinality of  $I_\sigma$ ; (44) minimizes the sum of distances between selected candidate nodes, in order to reduce the transportation time of MPSs and thus enhance DS restoration; (45) enforces one node to be selected from each PI that has at least one candidate node. Again, by the McCormick envelopes [22], terms  $\phi_i \cdot \phi_j$  can be equivalently linearized.

## VII. CASE STUDIES

In this section, the proposed co-optimization method for disaster recovery logistics is demonstrated on two systems. We use a computer with an Intel i5-4278U processor and 8GB memory. Involved MILP and IP problems are solved by Gurobi 7.5.2.

### A. Case I: IEEE 33-Node Test System

For this DS, we consider a scenario with 8 branches damaged by the natural disaster (see Fig. 2). The system has 2 depots and 2 RCs, i.e., RC 1 in depot 1 and RC 2 in depot 2. Resource capacity of RCs is set as 8. Both the number of resources and time periods required to repair different damaged components vary from 1 to 4. The DS also has 2 MPSs, i.e., 500 kW/400 kVar MEG 1, and 300 kW/300 kWh MESS 1. Priority weights of loads and the travel time/distance data are randomly generated. Branches 9-10, 9-15, 12-22, 14-15, 18-33 25-29, 28-29 and 30-31 are equipped with remote-controlled switches [24]. Some other data can be found in [20].

First, a minimal set of repair tasks is sought and pre-assigned to depots. The pre-assignment model (37)-(43) is solved within 0.13 s. Table I lists the results. In virtue of the back-up branches, i.e., the normally open branches, repairing 4 damaged branches is sufficient to fully restore all loads. The repair of the other 4 un-assigned damaged branches can be arranged later for an objective other than maximizing the sum of restored loads.

Second, candidate nodes for MPS connection are selected. Let  $N' = \{2, 5, 8, 15, 21, 29, 33\}$  be the set of all candidate nodes. Algorithm 1, which takes 0.14 s, accurately detects that the system is split into 4 PIs containing candidate nodes  $\{2\}$ ,  $\{5, 29\}$ ,  $\{8, 15, 21\}$  and  $\{33\}$ , respectively. Note that although these results are obvious in this case, Algorithm 1 is necessary to automatically generate such data for both small and large systems. Then, the candidate node selection problem (44)-(45) is solved in 0.04 s. Nodes  $\{2, 8, 29, 33\}$  are selected.

Third, after pre-assigning repair tasks and selecting candidate nodes, we solve the co-optimization problem. Let  $T = 12$  and  $\Delta t = 0.5$  hr; let  $vol_i = 2$  for all candidate nodes; let  $\alpha_{2,1}^s = 1$  for both MPSs. The co-optimization model is solved in 2.26 s. Table II and III list the dispatch of RCs and MPSs, respectively. Symbols “ $\rightarrow$ ” or “x” mean that this RC/MPS is being transported or has stopped working, respectively. MPSs change their locations only once for this small system. We will see more dynamic dispatch of MPSs in Case II. Fig. 4 depicts MPSs’ real power outputs. Table IV lists switch actions of the DS.

The proposed co-optimization method for disaster recovery logistics is also compared to other logistics strategies. As shown in Fig 5, the proposed method co-optimizing both RC dispatch and MPS dispatch with DS restoration has the best performance.

TABLE I  
PRE-ASSIGNMENT OF A MINIMAL SET OF REPAIR TASKS (CASE I)

	Depot 1	Depot 2
Pre-assigned repair tasks	branches 2-3, 5-6	branches 7-8, 30-31
Un-assigned repair tasks	branches 10-11, 16-17, 19-20, 9-15	

TABLE II  
ROUTING AND SCHEDULING OF RCs (CASE I)

RC	Time period	0	1	2~4	5~7	8~10	11~12
RC 1	Dispatch	depot 1	$\rightarrow$	branch 2-3	$\rightarrow$	branch 5-6	x
RC 2	Time period	0	1	2~3	4~5	6~7	8~12
	Dispatch	depot 2	$\rightarrow$	branch 7-8	$\rightarrow$	branch 30-31	x

TABLE III  
ROUTING AND SCHEDULING OF MPSs (CASE I)

MEG	Time period	0	1~3	4~10	11~12
MEG 1	Dispatch	node 2	$\rightarrow$	node 33	x
MESS	Time period	0	1~2	3~10	11~12
MESS 1	Dispatch	node 2	$\rightarrow$	node 29	x

TABLE IV  
DYNAMIC NETWORK RECONFIGURATION OF THE DS (CASE I)

Time period	3	4	11
Switch actions	close 25-29	close 8-21, 12-22, 18-33	open 28-29

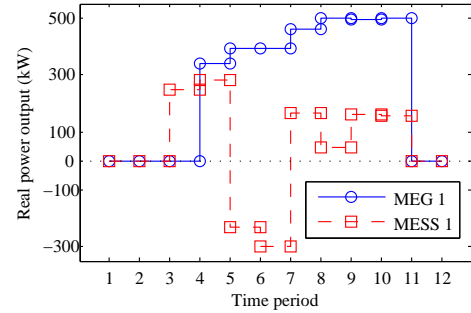


Fig. 4. Real power outputs of MPSs in each time period (Case I).

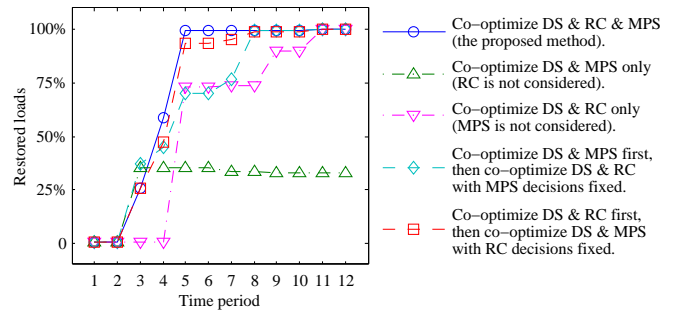


Fig. 5. Restored loads over time for different logistics strategies (Case I).

The recovery process is described in details by Fig. 6. At  $t = 3$ , MESS 1 arrives at and is connected to node 29. Closing branch 25-29, microgrid 1 is formed to restore nodes 3, 4, 6 and 30. At  $t = 4$ , with branch 7-8 repaired, microgrid 1 can further restore nodes 13 and 22 by closing branches 8-21 and 12-22. At  $t = 4$ , MEG 1 also arrives at and is connected to node 33. Closing branch 18-33, microgrid 2 is formed to restore all loads in it. At  $t = 5$ , with branch 2-3 repaired, microgrid 1 gets connected to the substation. Thus, MESS 1 can get charged at  $t = 5 \sim 6$  to supply future peak loads. At  $t = 8$ , with branch

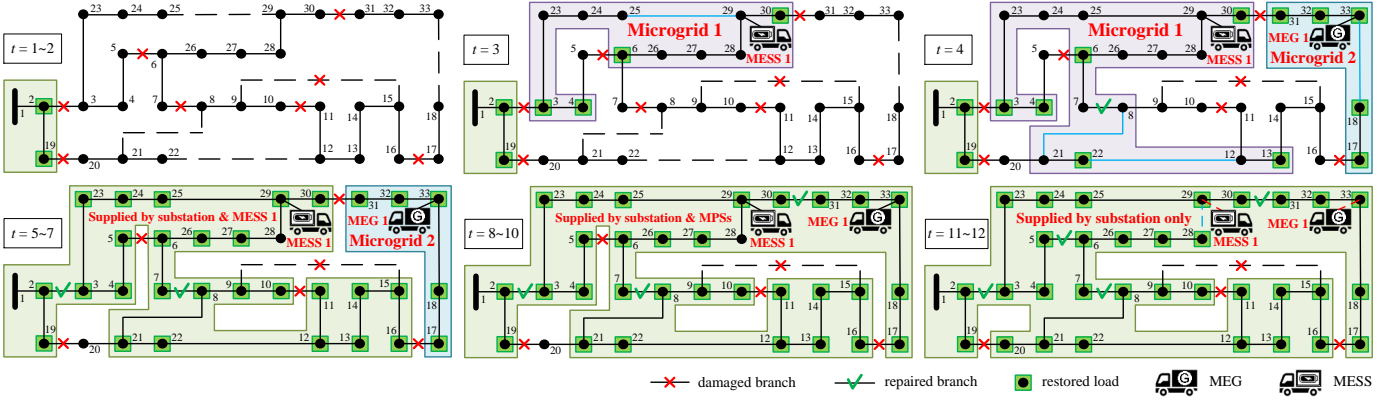


Fig. 6. DS service restoration process co-optimized with both RC dispatch and MPS dispatch (Case I).

TABLE V  
ROUTING AND SCHEDULING OF RCS (CASE II)

RC	Time period	0	1	2~4	5~6	7~9	10~11	12~13	14	15	16
RC 1	Dispatch	depot 1	→	branch 9-15	→	branch 72-73	→	branch 88-89	→	branch 106-107	x
	Time period	0	1	2~3	4	5	6	7	8~9	10~11	12~16
RC 2	Dispatch	depot 1	→	branch 103-108	→	branch 39-41	→	branch 15-56	→	branch 65-72	x
	Time period	0	1	2	3	4~5	6	7~8	9	10~11	12~16
RC 3	Dispatch	depot 2	→	branch 27-33	→	branch 92-93	→	branch 99-101	→	branch 17-19	x
	Time period	0	1	2~3	4	5	6	7~8	9~10	11~12	13~16
RC 4	Dispatch	depot 2	→	branch 43-45	→	branch 74-75	→	branch 25-26	→	branch 113-116	x
	Time period	0	1	2~3	4	5	6	7~8	9~10	11~12	13~16

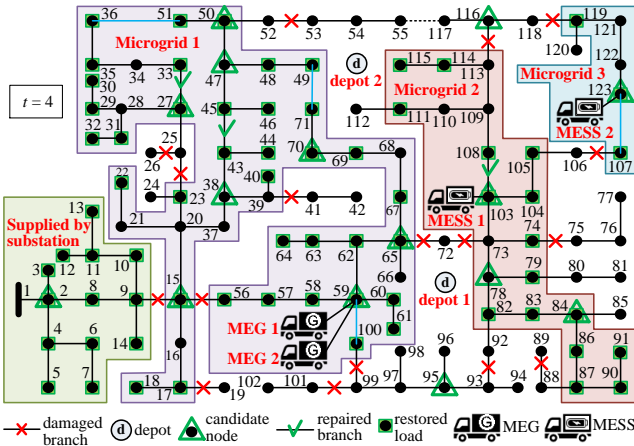


Fig. 7. IEEE 123-node test system and its restoration at  $t = 4$ .

30-31 repaired, microgrid 2 also gets connected to the main grid. However, due to operational constraints (low voltage of node 16 and large power flow on branch 24-25), nodes 20 and 28 cannot be restored until branch 5-6 is repaired at  $t = 11$ , when branch 28-29 is opened to avoid loop, and both MPSs are disconnected from the DS as they are no longer necessary.

### B. Case II: IEEE 123-Node Test System

A scenario with 20 branches damaged by the natural disaster is considered for the second test system in Fig. 7. It has 2 depots (each with 2 RCs), 4 MPSs (2 MEGs and 2 MESSs), and 12 branches equipped with remote-controlled switches [24]. Let  $T = 16$ . Some other data can be found in Case I or in [25].

First, the pre-assignment model (37)-(43) is solved in 0.43 s. Next, Algorithm 1 is run for 0.45 s, and the candidate node selection problem (44)-(45) is solved in 0.28 s. It selects nodes

TABLE VI  
ROUTING AND SCHEDULING OF MPSs (CASE II)

MEG	Time period	0	1~2	3~4	5	6~11	12~16
MEG 1	Dispatch	node 2	→	node 59	→	node 103	x
	Time period	0	1~2	3~4	5	6~11	12~16
MEG 2	Dispatch	node 2	→	node 59	→	node 103	→
	Time period	14~15	16	—			
MESS 1	Dispatch	node 123	x	—			
	Time period	0~1	2~3	4~5	6~7	8	9
MESS 2	Dispatch	node 116	x	—			
	Time period	10~12	13~16	—			
MESS 1	Dispatch	node 123	→	node 103	→	node 38	→
	Time period	0~1	15~16	—			
MESS 2	Dispatch	node 123	x	—			
	Time period	0~14	15~16	—			

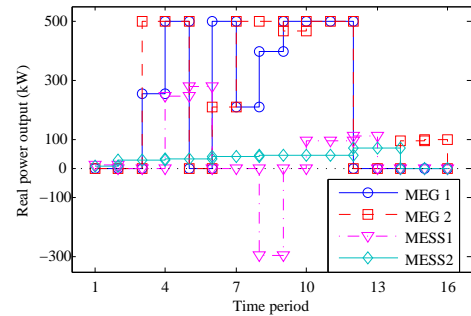


Fig. 8. Real power outputs of MPSs in each time period (Case II).

{2, 27, 38, 59, 95, 103, 116, 123}. At last, the co-optimization problem is solved in 1183 s. For space limit, we do not elaborate on the recovery process. Only the DS's restoration progress at  $t = 4$  is depicted in Fig 7 for illustration. Table V and VI list the dispatch of RCs and MPSs, respectively. Table V implicitly includes the results for the pre-assignment of a minimal set of repair tasks, too. Fig. 8 depicts real power outputs of MPSs.

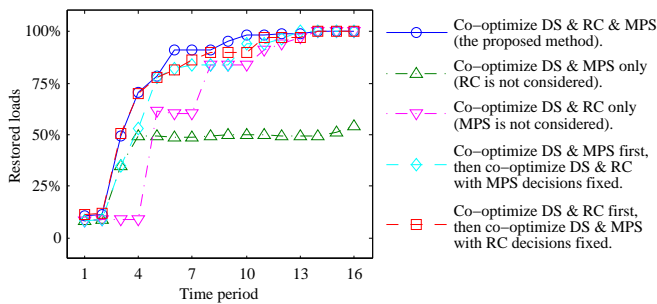


Fig. 9. Restored loads over time for different logistics strategies (Case II).

TABLE VII  
DYNAMIC NETWORK RECONFIGURATION OF THE DS (CASE II)

Time period	1	3	8	10
Switch actions	close 107-123	close 36-51, 49-71, 59-100	open 49-71	close 55-117

TABLE VIII  
COMPUTATION TIME OF THE CO-OPTIMIZATION PROBLEM (CASE I & II)

Solution methods	Case I	Case II
Proposed method	2.26 s	1183 s
Without any preprocessing	66.20 s	gap = 97.20% at 2 hr
Only with $N'$ reduced	37.59 s	gap = 59.92% at 2 hr
Only with all repairs pre-assigned	17.69 s	gap = 32.60% at 2 hr
Only with minimal repairs pre-assigned	6.67 s	gap = 5.34% at 2 hr

Table VII lists the DS's switch actions in its dynamic network reconfiguration. Fig. 9 again demonstrates the effectiveness and superiority of the proposed co-optimization method for disaster recovery logistics. The tables and figures indicate that, the proposed method is especially effective in coordinating RC dispatch and MPS dispatch to restore loads by dynamically forming microgrids in the DS. The microgrids are powered by MPSs, and reconfigured and extended by switch actions of the DS and repair actions of RCs.

### C. Computational Efficiency

Table VIII reports the computation time of different solution methods for the co-optimization model. For Case I, all methods attain the same solution. That is, preprocessing of the proposed method does not result in sub-optimality. For Case II, only the proposed method solves the co-optimization problem in 2 hr. Specifically, it is indicated that, compared to pre-assigning all repair tasks, pre-assigning a minimal set of repair tasks can better improve the computational efficiency.

## VIII. CONCLUSION

To enhance DS resilience, this paper builds a co-optimization method for disaster recovery logistics. RC dispatch, MPS dispatch and DS operation are jointly cooperated for electric service restoration. A MINLP model is formulated to attain resilient strategies that involve the routing and scheduling of RCs and MPSs, dynamic network reconfiguration of the DS, etc. The model is transformed into a MILP, and preprocessed to reduce computational complexity. Case studies demonstrate that the co-optimization method for disaster recovery logistics efficiently improves DS service restoration, especially by dynamic formation of microgrids that are powered by MPSs and topologized by repair actions of RCs and reconfiguration of the DS.

## REFERENCES

- [1] B. Zhou, D. Xu, C. Li, Y. Cao, K. W. Chan, Y. Xu, and M. Cao, "Multi-objective generation portfolio of hybrid energy generating station for mobile emergency power supplies," *IEEE Trans. Smart Grid*, in press (early access).
- [2] "Transportable energy storage systems project," Elect. Power Res. Inst., Palo Alto, CA, USA, Tech. Rep. 1017818, Oct. 2009.
- [3] C. Chen, J. Wang, F. Qiu, and D. Zhao, "Resilient distribution system by microgrids formation after natural disasters," *IEEE Trans. Smart Grid*, vol. 7, no. 2, pp. 958–966, Mar. 2016.
- [4] T. Ding, Y. Lin, G. Li, and Z. Bie, "A new model for resilient distribution systems by microgrids formation," *IEEE Trans. Power Syst.*, vol. 32, no. 5, pp. 4145–4147, Sep. 2017.
- [5] P. Toth and D. Vigo, *The Vehicle Routing Problem*, Philadelphia, PA: SIAM, 2002.
- [6] N. Perrier, B. Agard, P. Baptiste, J.-M. Frayret, A. Langevin, R. Pellerin, D. Riopel, and M. Trépanier, "A survey of models and algorithms for emergency response logistics in electric distribution systems. Part I: Reliability planning with fault considerations," *Comput. Oper. Res.*, vol. 40, no. 7, pp. 1895–1906, Jul. 2013.
- [7] —, "A survey of models and algorithms for emergency response logistics in electric distribution systems. Part II: Contingency planning level," *Comput. Oper. Res.*, vol. 40, no. 7, pp. 1907–1922, Jul. 2013.
- [8] K. G. Zografos, C. Douligeris, and P. Tsoumpas, "An integrated framework for managing emergency-response logistics: the case of the electric utility companies," *IEEE Trans. Eng. Manag.*, vol. 45, no. 2, pp. 115–126, May 1998.
- [9] A. Arif, Z. Wang, J. Wang, and C. Chen, "Power distribution system outage management with co-optimization of repairs, reconfiguration, and dg dispatch," *IEEE Trans. Smart Grid*, in press (early access).
- [10] H. H. Abdeltawab and Y. A.-R. I. Mohamed, "Mobile energy storage scheduling and operation in active distribution systems," *IEEE Trans. Ind. Electron.*, vol. 64, no. 9, pp. 6828–6840, Sep. 2017.
- [11] Y. Chen, Y. Zheng, F. Luo, J. Wen, and Z. Xu, "Reliability evaluation of distribution systems with mobile energy storage systems," *IET Renew. Power Gener.*, vol. 10, no. 10, pp. 1562–1569, Nov. 2016.
- [12] H. Gao, Y. Chen, S. Mei, S. Huang, and Y. Xu, "Resilience-oriented pre-hurricane resource allocation in distribution systems considering electric buses," *Proc. IEEE*, vol. 105, no. 7, pp. 1214–1233, Jul. 2017.
- [13] S. Lei, J. Wang, C. Chen, and Y. Hou, "Mobile emergency generator repositioning and real-time allocation for resilient response to natural disasters," *IEEE Trans. Smart Grid*, vol. 9, no. 3, pp. 2030–2041, May 2018.
- [14] G. B. Dantzig and J. H. Ramser, "The truck dispatching problem," *Manag. Sci.*, vol. 6, no. 1, pp. 80–91, Oct. 1959.
- [15] A. J. Miller and L. A. Wolsey, "Tight formulations for some simple mixed integer programs and convex objective integer programs," *Math. Program.*, vol. 98, no. 1, pp. 73–88, Sep. 2003.
- [16] S. Iwai, T. Kono, M. Hashiwaki, and Y. Kawagoe, "Use of mobile engine generators as source of back-up power," in *Proc. IEEE 31st Int. Telecom. Energy Conf.*, Incheon, South Korea, Oct. 2009, pp. 1–6.
- [17] R. A. Jabr, R. Singh, and B. C. Pal, "Minimum loss network reconfiguration using mixed-integer convex programming," *IEEE Trans. Power Syst.*, vol. 27, no. 2, pp. 1106–1115, May 2012.
- [18] H. Ahmadi and J. R. Marti, "Mathematical representation of radiality constraint in distribution system reconfiguration problem," *Int. J. Electr. Power Energy Syst.*, vol. 64, pp. 293–299, Jan. 2015.
- [19] P. C. Pop, "The generalized minimum spanning tree problem," Ph.D. dissertation, Twente Univ. Press, Enschede, The Netherlands, 2002.
- [20] M. E. Baran and F. F. Wu, "Network reconfiguration in distribution systems for loss reduction and load balancing," *IEEE Trans. Power Del.*, vol. 4, no. 2, pp. 1401–1407, Apr. 1989.
- [21] J. A. Taylor and F. S. Hover, "Convex models of distribution system reconfiguration," *IEEE Trans. Power Syst.*, vol. 27, no. 3, pp. 1407–1413, Aug. 2012.
- [22] G. P. McCormick, "Computability of global solutions to factorable non-convex programs: Part I—convex underestimating problems," *Math. Program.*, vol. 10, no. 1, pp. 147–175, Dec. 1976.
- [23] X. Chen, W. Wu, and B. Zhang, "Robust restoration method for active distribution networks," *IEEE Trans. Power Syst.*, vol. 31, no. 5, pp. 4005–4015, Sep. 2016.
- [24] S. Lei, J. Wang, and Y. Hou, "Remote-controlled switch allocation enabling prompt restoration of distribution systems," *IEEE Trans. Power Syst.*, vol. 33, no. 3, pp. 3129–3142, May 2018.
- [25] IEEE PES Power System Analysis, Computing and Economics Committee, *IEEE 123 Node Test Feeder*, Feb. 2014. [Online]. Available: <http://ewh.ieee.org/soc/pes/dsacom/testfeeders/feeder123.zip>